

Contents

1	Introduction	7
1.1	Interferometer as a gravitational wave detector	8
1.2	Quantum Noise	10
1.2.1	Quantized fields	10
1.2.2	Noise in the sideband picture	11
1.2.3	Quadrature operators and variances	13
1.2.4	Uncertainty relation	15
1.2.5	Vacuum and coherent states	15
1.2.6	Phase space representation of quantum fields	18
1.3	Quantum noise in interferometers	19
1.4	Squeezed States	24
1.4.1	Two Photon Coherent States	24
1.4.2	Photon statistics	26
1.4.3	Squeezing operator	26
1.4.4	Squeezed vacuum state	27

List of Figures

1-1	Simple Michelson interferometer	8
1-2	Amplitude and phase noise in the sideband picture	12
1-3	Amplitude and phase modulation in the electric field quadratures	13
1-4	Vacuum fluctuations at every sideband frequency add quantum noise to the electromagnetic field.	16
1-5	Q representation of ground state and coherent state	20
1-6	Input and output fields of a Michelson interferometer	20
1-7	Advanced LIGO Quantum Noise	23
1-8	Quadrature variances of two photon states with $\beta = 0$ and $\tanh \zeta = 0.4$ as θ varies. When the variance of one quadrature is less than one, the other quadrature has increased variance. When θ is an integral multiple of π , the state is a minimum uncertainty state, and the product of the variances in the two quadratures is one.	25
1-9	Q-representation of squeezed states	28

List of Tables

Chapter 1

Introduction

Einstein used his theory of general relativity to predict the existence of gravitational waves almost a century ago. Direct detection of gravitational waves would provide a new way of observing the universe. Gravitational waves interact incredibly weakly with matter. This means that they are unaffected by passing through the dense ionized gases that obscure violent explosions and the early universe to electromagnetic observations. This means that gravitational waves could provide rich new insight into events that are currently difficult to study. The weakness of the interaction with matter also means that direct detection is a tremendous challenge. A passing gravitational wave induces a strain in any object it passes through, alternately stretching and squeezing the object along orthogonal axes by an amount proportional to the length of the object: $h = \Delta L/L$. For the events that earth based detectors aim to observe the expected strain are on the order of 10^{-21} . This means that a large part of the effort to detect gravitational waves is aimed at reducing noise in the detectors to improve their sensitivity. This thesis is about a technique to reduce the noise caused by the quantum nature of light. We reduced the noise of an Enhanced LIGO interferometer by injecting quantum squeezing.

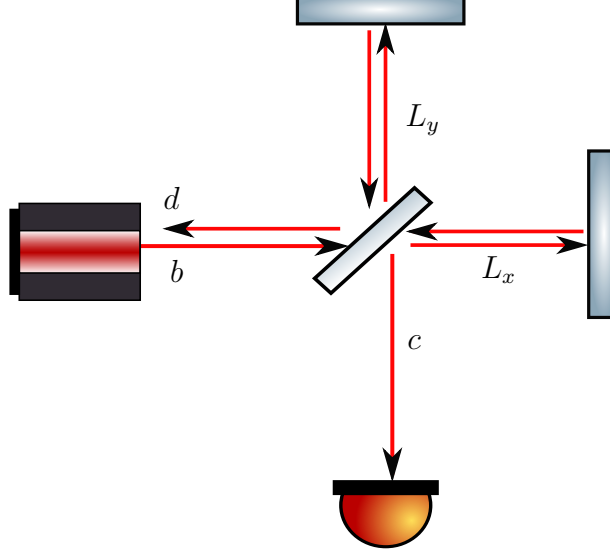


Figure 1-1: Simple Michelson interferometer

1.1 Interferometer as a gravitational wave detector

The simple Michelson interferometer illustrated in 1-1 can be used to measure the strain induced by a passing gravitational wave of the correct polarization. Laser light at the frequency ω enters the interferometer where it is split by a beam splitter and sent down two orthogonal arms. The beam-splitter is represented by the transformation from its input fields to its output fields using the convention of [14, p 407]:

$$\mathbf{out} = (\mathbf{BS}) \mathbf{in} \quad \mathbf{BS} = \frac{1}{\sqrt{2}} \begin{pmatrix} 1 & i \\ i & 1 \end{pmatrix} \quad (1.1)$$

It each arm the light acquires a phase shift as it travels to the end mirror and back, we will call the phase shift ϕ_x or ϕ_y , they are proportional to the lengths of the two arms, L_x, L_y . A passing gravitational wave with the optimal polarization changes the phases by [15]:

$$\begin{aligned} \phi_x &= \frac{2\omega L_x}{c} \left(1 + \frac{h_+}{2} \right) \\ \phi_y &= \frac{2\omega L_y}{c} \left(1 - \frac{h_+}{2} \right) \end{aligned} \quad (1.2)$$

Writing the arm lengths in terms of common and differential parts, $L_x = L + l$ and $L_y = L - l$ the phases can also be written in terms of common and differential parts:

$$\begin{aligned}\phi_x &= \Phi + \phi & \Phi &= \frac{2\omega}{c} \left(L + \frac{lh_+}{2} \right) \\ \phi_y &= \Phi - \phi & \phi &= \frac{2\omega}{c} \left(l + \frac{Lh_+}{2} \right)\end{aligned}\tag{1.3}$$

And the propagation down the arms and back toward the beam-splitter is represented by:

$$\mathbf{A} = e^{i\Phi} \begin{pmatrix} e^{i\phi} & 0 \\ 0 & e^{-i\phi} \end{pmatrix}\tag{1.4}$$

Now the interferometer output in terms of the input field is:

$$\begin{aligned}\mathbf{out} &= (\mathbf{BS})\mathbf{A}(\mathbf{BS})\mathbf{in} \\ \begin{pmatrix} c \\ d \end{pmatrix} &= e^{i(\Phi+\pi/2)} \begin{pmatrix} \sin \phi & \cos \phi \\ \cos \phi & -\sin \phi \end{pmatrix} \begin{pmatrix} 0 \\ b \end{pmatrix}\end{aligned}\tag{1.5}$$

The photo-current measured by the detectors at the anti-symmetric port (c) and the reflected port is:

$$\begin{aligned}P_{as} &\propto |c|^2 = |b|^2 \cos^2 \phi \\ P_{refl} &\propto |d|^2 = |b|^2 \sin^2 \phi\end{aligned}\tag{1.6}$$

The differential arm length l sets the ratio of the power at the antisymmetric port to the reflected power, the operating point where no light exits the anti-symmetric port is called the dark fringe. The interferometers are operated near this point, so $l = (\pi/2 + \Delta)c/2\omega$. Using the small angle approximation, the power at the antisymmetric port is:

$$P_{as} \propto |b|^2 \left(\Delta^2 + \frac{2\Delta\omega L}{c} h_+ \right)\tag{1.7}$$

At this operating point the power at the dark port has a linear dependence on the gravitational wave strain. The goal of a worldwide network of interferometers is to measure a time series of the power at the anti-symmetric port, and find evidence of a passing gravitational wave. Because the strains expected are so small, on the order of 10^{-21} , the noise requirements for gravitational wave interferometers are very stringent. The main limiting noise sources in current gravitational wave detectors are seismic noise, thermal noise, and shot noise. Shot noise is one form of quantum noise, caused by the quantum nature of light. In the next generation of gravitational waves quantum noise is expected to limit the sensitivity in most of the sensitive band.

1.2 Quantum Noise

1.2.1 Quantized fields

The quantized electric field in a single mode is written in terms of annihilation and creation operators [9]:

$$E(t) = \varepsilon_0 (a(t)e^{-i\omega t} + a^\dagger(t)e^{i\omega t}) \quad (1.8)$$

The factor ε_0 is a normalization factor with dimensions of electric field, in SI units it is given by $\sqrt{\hbar\omega/\epsilon_0 V}$ where V is the volume of the mode and ϵ_0 is the permittivity of free space [9]. This electric field operator is a Heisenberg picture operator which contains the full time evolution of the system. In free space, or an empty cavity without losses, the annihilation and creation operators here would be Schrödinger picture operators with no time dependence. By allowing the annihilation and creating operators to have time dependence we can take into account interactions, and describe noise on the field. The time dependent annihilation and creation operators we have used are in the rotating frame at the optical frequency ω . Inside of optical cavities the field only resonates when the round trip length (perimeter) of the cavity is an integral number of wavelengths, so the mode frequencies are discrete. The

carrier frequency ω is the cavity resonance frequency:

$$\omega = \omega_{a,n} = \frac{2\pi c}{n\lambda} \quad (1.9)$$

where n is an integer. The Hamiltonian for this field is $H = \hbar\omega_a a^\dagger(t)a(t)$.

Outside of a cavity, the mode volume becomes infinite and there are a continuum of modes at every frequency. One convention for modes in free space is to write the normalization factor as $\varepsilon_0 = \sqrt{\hbar\omega/\epsilon_0 c A}$ where A is the area of the mode, then the units of the annihilation and creation operators in the time domain are $\sqrt{\# \text{ photons/sec}}$ [11]. This can be a source of confusion because the annihilation and creation operators inside of a cavity are unitless ($\sqrt{\# \text{ photons}}$) inside of a cavity and have units outside.

1.2.2 Noise in the sideband picture

Both classical and quantum noise on an optical field can be understood in terms of sidebands, or in terms of noise quadratures. A field with a carrier frequency ω has noise at the frequency Ω . If the field is amplitude modulated it becomes:

$$(1 + \Gamma \cos \Omega t) E e^{i\omega t} + h.c. = E e^{i\omega t} + \frac{\Gamma E}{2} e^{i(\omega+\Omega)t} + \frac{\Gamma E}{2} e^{i(\omega-\Omega)t} + h.c. \quad (1.10)$$

$$= (\bar{E} + \delta E(t)) e^{i\omega t} + h.c. \quad (1.11)$$

A phase modulated field becomes:

$$E e^{i\omega t + \Gamma \cos \Omega t} + h.c. = E e^{i\omega t} + \frac{i\Gamma E}{2} e^{i(\omega+\Omega)t} + \frac{i\Gamma E}{2} e^{i(\omega-\Omega)t} + h.c. \quad (1.12)$$

$$= (\bar{E} + \delta E(t)) e^{i\omega t} + h.c. \quad (1.13)$$

In both cases the noise can be attributed to symmetric sidebands at the frequencies $\omega \pm \Omega$ around the carrier. The phase relationship between the sidebands and the carrier determines whether the noise is amplitude noise or phase noise. Amplitude noise is described by the real part of $\delta E/\bar{E}$, while phase noise is described by the imaginary part.

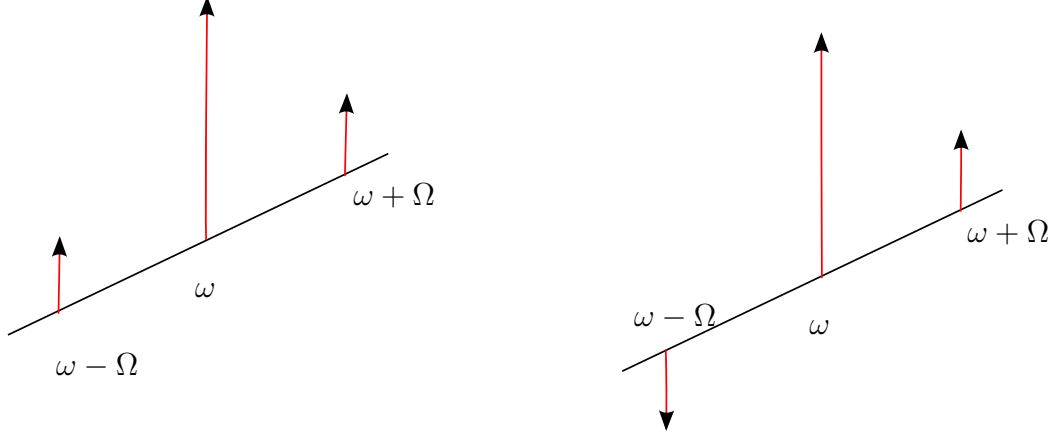


Figure 1-2: Phasors of amplitude noise (left) and phase noise (right) in the sideband picture. In the frame rotating at the carrier frequency ω the carrier is still in these diagrams while the sidebands rotate at Ω , the signal at $\omega + \Omega$ rotating clockwise while the idler at $\omega - \Omega$ rotates counter clockwise. (Sidebands have equal amplitudes)

We can describe any noisy field as the sum of sidebands at different frequencies by writing the annihilation operator in terms of Fourier components.

$$a(t) = \int_{-\infty}^{\infty} \frac{d\Omega}{\sqrt{2\pi}} \tilde{a}(\Omega) e^{i\Omega t} \quad (1.14)$$

Using the convention that $a^\dagger(t) = [a(t)]^\dagger$ we have $[a(\Omega)]^\dagger = a^\dagger(-\Omega)$ [4, 8, p440]. Using 1.8 the quantized electric field in terms of these Fourier components is:

$$E(t) = \frac{\varepsilon_0}{\sqrt{2\pi}} \int_{-\infty}^{\infty} d\Omega [\tilde{a}(\Omega) e^{-i(\omega+\Omega)t} + \tilde{a}^\dagger(-\Omega) e^{i(\omega+\Omega)t}] \quad (1.15)$$

The operators $\tilde{a}(\Omega)$ and $\tilde{a}^\dagger(-\Omega)$ represent positive and negative frequency sidebands around the carrier frequency. This would be more apparent if we had not separated out the time dependence at the carrier frequency in 1.8, in that case by the translation property of Fourier transforms would give us 1.15 as:

$$E(t) = \frac{\varepsilon_0}{\sqrt{2\pi}} \int_{-\infty}^{\infty} d\Omega [\tilde{a}(\omega + \Omega) e^{-i\Omega t} + \tilde{a}^\dagger(\omega - \Omega) e^{i\Omega t}] \quad (1.16)$$

Sometimes the limits of the integral only include positive frequencies, as in the papers in-

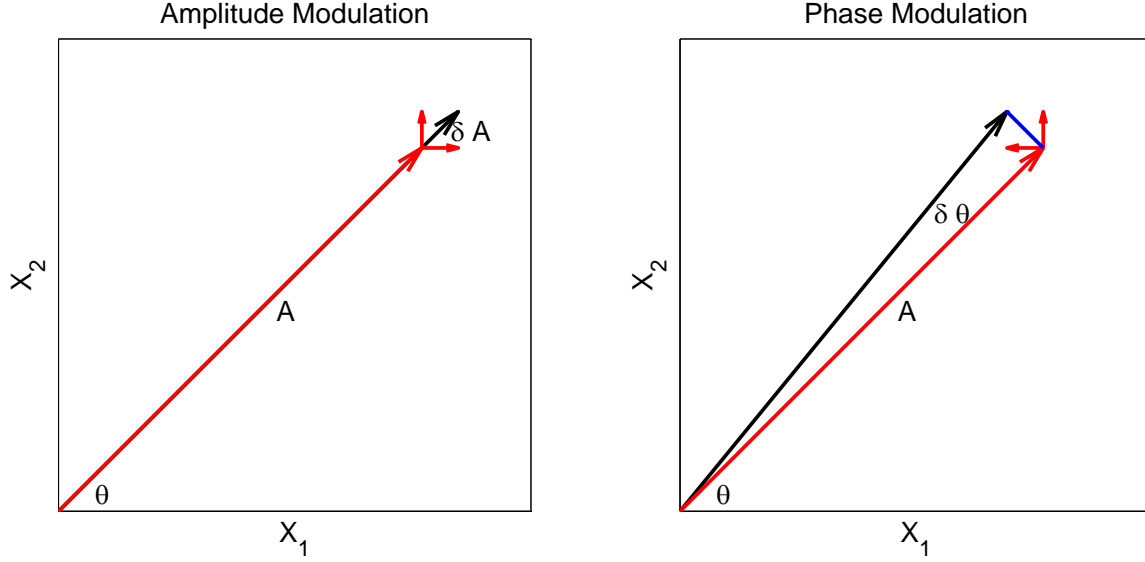


Figure 1-3: The same fields as shown in 1-2 one eighth of a cycle later at $t = \pi/4\Omega$, plotted in the plane of X_1 and X_2 . In this plane, the polar coordinate represents the phase of the field while the radial coordinate is the amplitude. In the rotating frame, the carrier field has a constant phase while upper and lower sidebands rotate around it at Ω in opposite directions. Each of the individual frequency components is shown in red while the total field is shown in black. In the case of amplitude modulation the sidebands add only amplitude noise to the carrier, while in the case of phase modulation the phases are arranged so that only phase noise is added.

roducing the two photon formalism by Caves and Schumaker [3, 12]. In this thesis the transformation to the Fourier domain will be a Fourier transform over all frequencies, following Collet and Gardiner [4, 7].

1.2.3 Quadrature operators and variances

We can also write the field as the sum of two quadratures:

$$E(t) = \varepsilon_0 (X_1(t) \cos \omega t + X_2(t) \sin \omega t) \quad (1.17)$$

These two quadratures can be written in terms of static and fluctuating parts: $X_{1,2} = \bar{X}_{1,2} + \delta X_{1,2}(t)$. The static part describes the carrier while the fluctuating part describes

a modulation. Figure 1-2 and 1-3 show amplitude and phase modulation represented by frequency components and in the two quadratures. Comparing 1.17 and 1.8 the quadrature operators are:

$$X_1(t) = (a(t) + a^\dagger(t)) \quad (1.18)$$

$$X_2(t) = -i(a(t) - a^\dagger(t)) \quad (1.19)$$

We can define an arbitrary quadrature operator [1, p 6]:

$$X(\theta) = X_1(t) \cos \theta + X_2(t) \sin \theta \quad (1.20)$$

$$= a(t)e^{i\theta} + a^\dagger(t)e^{-i\theta} \quad (1.21)$$

If we set θ to the phase of the carrier, then $\delta X(\theta)$ is amplitude noise while $\delta X(\theta + \pi/2)$ is phase noise. The quadrature operators can be written in the frequency domain by taking a Fourier transform:

$$\tilde{X}_{1,2}(\Omega) = \frac{1}{\sqrt{2\pi}} \int_{-\infty}^{\infty} d\Omega e^{i\Omega t} X_{1,2}(t) \quad (1.22)$$

In the frequency domain the transformation from the annihilation operators to the quadrature operators is the same as in the time domain:

$$\begin{pmatrix} \tilde{X}_1(\Omega) \\ \tilde{X}_2(\Omega) \end{pmatrix} = \begin{pmatrix} 1 & 1 \\ -i & i \end{pmatrix} \begin{pmatrix} \tilde{a}(\Omega) \\ \tilde{a}^\dagger(-\Omega) \end{pmatrix}$$

$$\tilde{\mathbf{X}} = \mathbf{R}\tilde{\mathbf{a}} \quad (1.23)$$

The arbitrary quadrature operator in the frequency domain is:

$$\tilde{X}(\Omega, \theta) = \tilde{a}(\Omega)e^{i\theta} + \tilde{a}^\dagger(-\Omega)e^{-i\theta} \quad (1.24)$$

The quadrature variances are the quantities that we normally measure. Measurements always

have a finite bandwidth, w , which is normalized out of the power spectral density [1, p13]:

$$S(\theta, \Omega) = \frac{1}{w} \int_{-w/2}^{w/2} \int_{-\infty}^{\infty} \langle X(\theta, \Omega) X^\dagger(\theta, \Omega') \rangle d\Omega' d\Omega$$

$$S(\theta, \Omega) = \langle |\tilde{X}(\theta, \Omega)|^2 \rangle = V(\theta, \Omega) \quad (1.25)$$

which is the variance of $\tilde{X}(\Omega)$. This measurement is made by integrating the noise in a frequency band called the resolution bandwidth, which is then normalized out. 1.25 only holds if the noise is constant over the resolution bandwidth of the measurement.

1.2.4 Uncertainty relation

There is an uncertainty relation between orthogonal quadratures of the electromagnetic field. Using the commutation relations for annihilation and creation operators, $[a, a^\dagger] = 1$, the commutation relation for the single mode quadrature operators is:

$$[X_1, X_2] = 2i \quad (1.26)$$

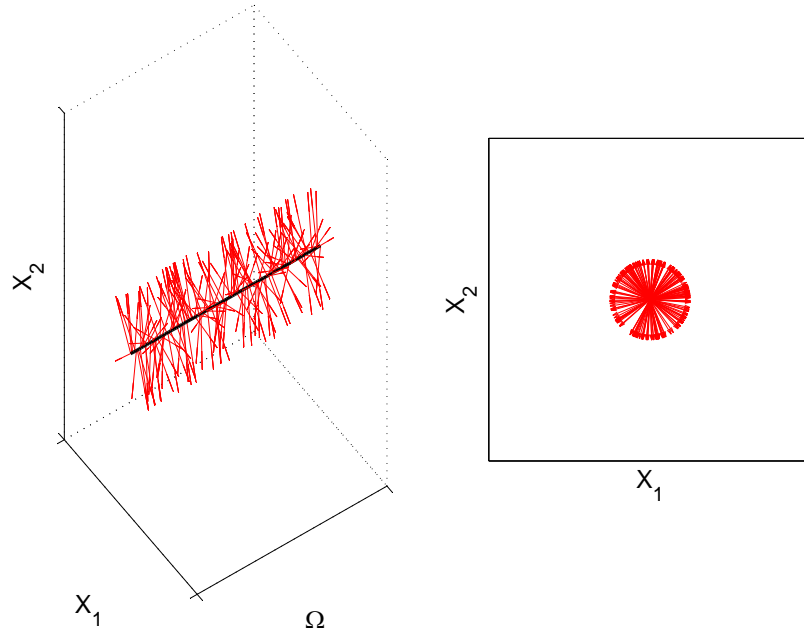
Which means the uncertainties are governed by:

$$\Delta X_1 \Delta X_2 \geq 1 \quad (1.27)$$

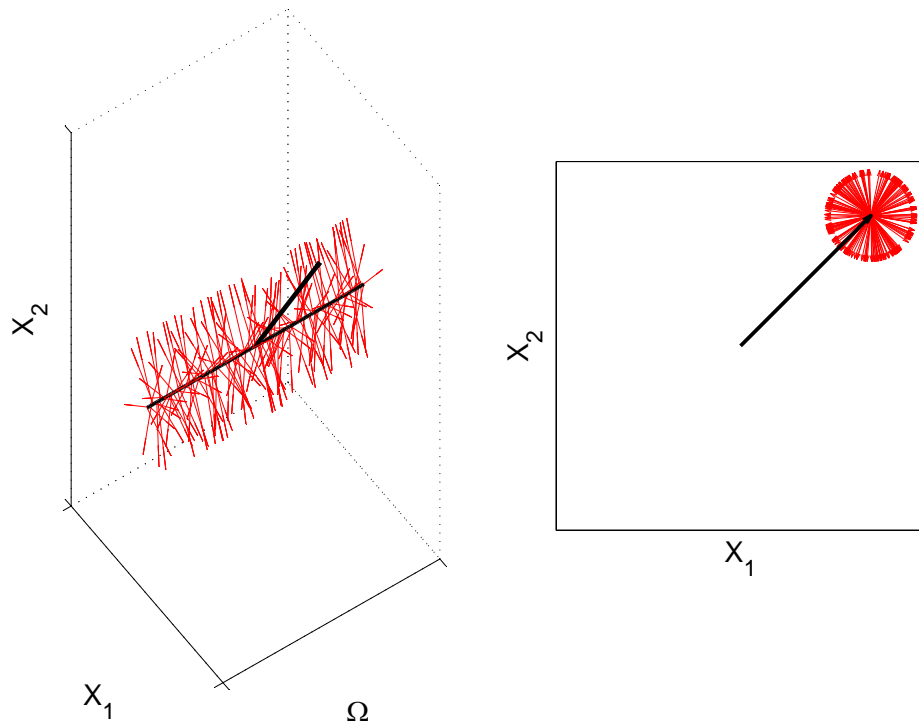
The variance of these quadrature operators are measured in the frequency domain by a power spectral density, the uncertainty relation in the frequency domain is:

$$V(\theta, \Omega) V(\theta + \pi/2, \Omega) \geq 1 \quad (1.28)$$

1.2.5 Vacuum and coherent states



(a) Semiclassical representation of the ground state.



(b) Semiclassical representation of the coherent state.

Figure 1-4: Vacuum fluctuations at every sideband frequency add quantum noise to the electromagnetic field.

The ground state and coherent state of the electromagnetic field can be understood as the sum of uncorrelated sidebands. Due to vacuum fluctuations there is a finite probability of having a single photon at each sideband frequency with a random phase, as shown in 1-4a. The total field is the sum of all these sidebands. Since the fluctuations are random and uncorrelated, we would expect a probability distribution for the total field would be a Gaussian centered at the origin in the plane of X_1, X_2 , with equal variance in the two quadratures.

The coherent states are eigenstates of the single mode annihilation operator:

$$a |\alpha\rangle = \alpha |\alpha\rangle \quad (1.29)$$

The ground state is also a coherent state, with eigenvalue 0. We can expand the state α in terms of number states and use the eigenvalue equation to find a recursion relation for the coefficients:

$$\begin{aligned} a \sum_{n=0}^{\infty} c_n |n\rangle &= \alpha \sum_{n=0}^{\infty} c_n |n\rangle \\ c_{n+1} &= \frac{\alpha}{\sqrt{n+1}} c_n \end{aligned} \quad (1.30)$$

Using the normalization to find $|c_0|^2 = e^{-|\alpha|^2}$ we have found the coherent states in the basis of number states.

$$|\alpha\rangle = e^{-|\alpha|^2/2} \sum_{n=0}^{\infty} \frac{\alpha^n}{\sqrt{n!}} |n\rangle \quad (1.31)$$

For a coherent state $|\alpha|^2 = \langle n \rangle$, so photon number measurements on a coherent state would give a Poisson distribution [10]:

$$P_n = |c_n|^2 = e^{-\langle n \rangle} \frac{\langle n \rangle^n}{n!} \quad (1.32)$$

Using the fact that the number states are generated by: $|n\rangle = a^{\dagger n}/\sqrt{n!}|0\rangle$:

$$|\alpha\rangle = e^{-|\alpha|^2/2} \sum_{n=0}^{\infty} \frac{(\alpha a^{\dagger})^n}{n!} |0\rangle = e^{-|\alpha|^2/2} e^{\alpha a^{\dagger}} |0\rangle \quad (1.33)$$

We can write the vacuum state as $|0\rangle = e^{-\alpha^* a} |0\rangle$, and then we have [13]:

$$|\alpha\rangle = e^{-|\alpha|^2/2} e^{\alpha a^{\dagger}} e^{-\alpha^* a} |0\rangle = D(\alpha) |0\rangle \quad (1.34)$$

The Baker Hausdorff formula can be used to write the displacement operator $D(\alpha)$ in the more familiar form:

$$D(\alpha) = e^{(\alpha a^{\dagger} - \alpha^* a)} \quad (1.35)$$

This operator is the generator of the coherent states, it is a displacement operator in the sense that $D^{-1}(\alpha)aD(\alpha) = a + \alpha$. A classical harmonic oscillator starting at rest at the equilibrium position (its ground state) can be put into a excited state by displacing the mass. The quantum coherent states are the closest quantum approximation to these classical states and can also be generated by displacing the ground state, using $D(\alpha)$.

The quadrature variances of a coherent state are:

$$\begin{aligned} V_1 &= \langle \alpha | X_1^2 | \alpha \rangle - \langle \alpha | X_1 | \alpha \rangle^2 = 1 \\ V_2 &= \langle \alpha | X_1^2 | \alpha \rangle - \langle \alpha | X_1 | \alpha \rangle^2 = 1 \end{aligned} \quad (1.36)$$

These are minimum uncertainty states which satisfy the equality of the uncertainty principle: $V_1 V_2 = 1$.

1.2.6 Phase space representation of quantum fields

The plane of X_1 and X_2 from Figure 1-3 is a phase space for a classical field. We would like to represent a quantum state as a distribution in phase space, using the plane of X_1, X_2 .

The expectation values for the quadrature amplitudes for a coherent state are:

$$X_1 = \langle \alpha | \frac{a + a^\dagger}{2} | \alpha \rangle = \text{Re}[\alpha] \quad (1.37)$$

$$X_2 = \langle \alpha | \frac{a - a^\dagger}{2i} | \alpha \rangle = \text{Im}[\alpha] \quad (1.38)$$

To represent a state in the plane of X_1, X_2 it is natural to use the basis of coherent states. Coherent states are an over-complete basis, any state can be represented as a linear combination of coherent states but the coherent states are not orthogonal. This means that in this phase space the coherent states will not be points, but will have a finite width, representing the variances of $X_{1,2}$. One quasi-probability distribution we can use is the Q representation:

$$Q(\alpha) = \langle \alpha | \rho | \alpha \rangle / \pi \quad (1.39)$$

where ρ is the density matrix. The Q function is normalized and always positive, $\int Q(\alpha) d^2\alpha = 1$, as a classical phase space probability distribution would be. The Q representation of a coherent state $|\beta\rangle$ is:

$$Q(\alpha) = \frac{1}{\pi} e^{-|\beta - \alpha|^2} \quad (1.40)$$

These are Gaussian states, with a Gaussian quasi-probability distribution centered around β , with equal widths in both quadratures. This quasi-probability distribution for the vacuum or ground state and a coherent state are shown in Figure1-5. There several similar phase space representations of quantum states, the most commonly used are the P representation and the Wigner function.

1.3 Quantum noise in interferometers

There are two dominant types of quantum noise in an interferometer with suspended mirrors, shot noise and quantum radiation pressure noise. Shot noise can be understood by the

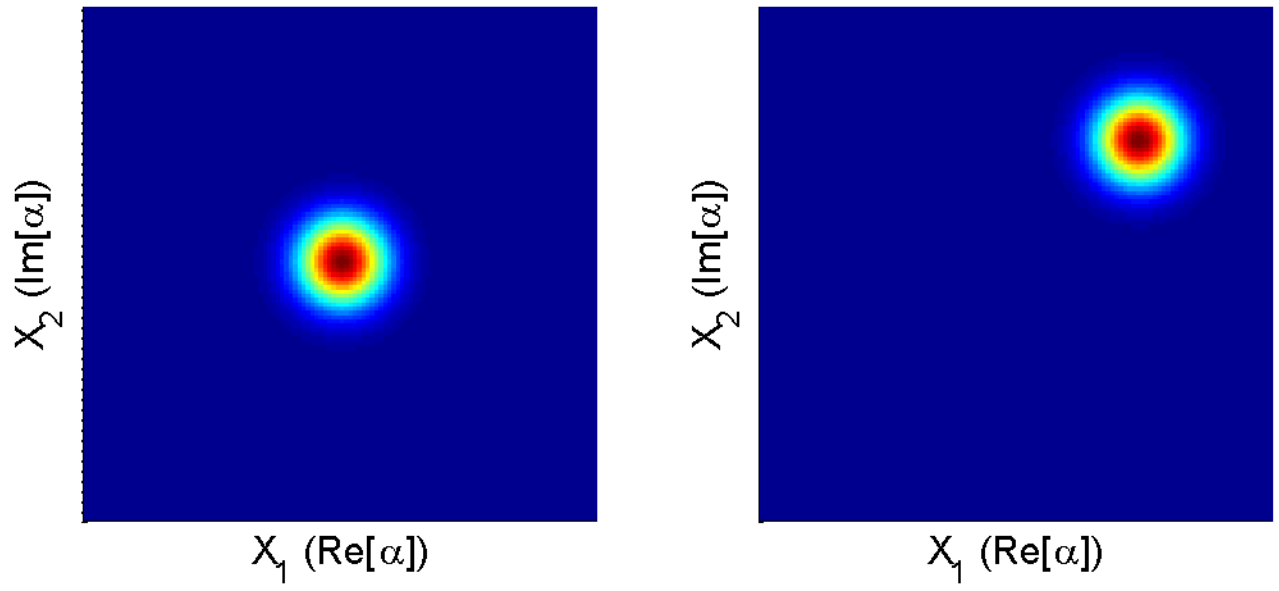


Figure 1-5: Q representation of ground state and coherent state

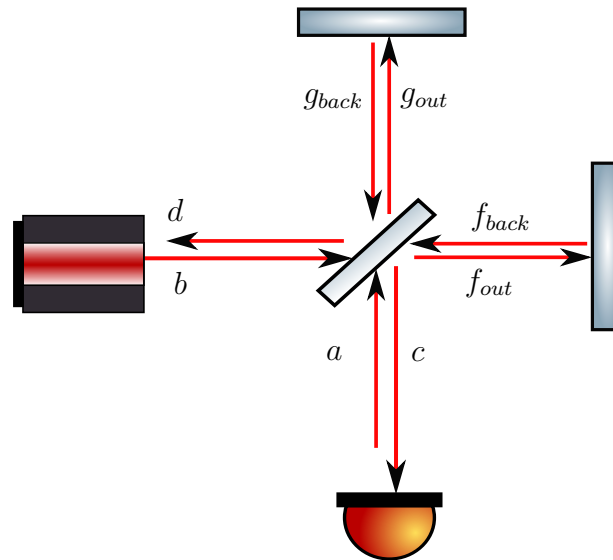


Figure 1-6: Input and output fields of a Michelson interferometer

random arrival times of photons at the photodetector, while radiation pressure noise can be understood as motion of the mirrors caused by fluctuations in the radiation pressure on the mirrors due to amplitude fluctuations in the arms. To understand the quantum behavior of the interferometer, we need to take into account vacuum fields that we ignored in 1.1. Figure 1-6 shows a diagram of a gravitational wave interferometer including the input field that enters from the anti-symmetric port. Caves pointed out that both kinds of quantum noise are caused by vacuum fluctuations entering at the dark port [2].

The fields in the interferometer arms, which cause the radiation pressure on each of the end mirrors are given by:

$$\begin{pmatrix} g_{out} \\ f_{out} \end{pmatrix} = \frac{1}{\sqrt{2}} \begin{pmatrix} 1 & i \\ i & 1 \end{pmatrix} \begin{pmatrix} a \\ b \end{pmatrix} \quad (1.41)$$

The difference between the radiation pressure in the two arms can cause a change in l which can mimic a gravitational wave signal [2]:

$$\begin{aligned} \mathcal{P} &\propto f_{out}^\dagger f_{out} - g_{out}^\dagger g_{out} \\ &\propto i(b^\dagger a - a^\dagger b) \end{aligned} \quad (1.42)$$

Since b is the field of the input laser, we can assume that it is in a coherent state with a large amplitude, and replace b by $|\beta|e^{i\theta_b}$. The differential radiation pressure is then:

$$\mathcal{P} \propto |\beta| \left(a e^{i(\pi/2 - \theta_b)} + a^\dagger e^{-i(\pi/2 - \theta_b)} \right) = |\beta| X_a(\pi/2 - \theta_b) \quad (1.43)$$

Where $X_a(\theta)$ is the arbitrary quadrature operator for a , the quantum fluctuations that enter at the dark port. The variance of \mathcal{P} , which is proportional to the variance of the quantum fluctuations entering at the dark port, scaled by the laser power $|\beta|^2$, causes the radiation pressure noise. Since \mathcal{P} is a force on the suspended mirrors which are harmonic oscillators in the earth's gravitational field, the radiation pressure noise is filtered by the frequency response of a single pendulum. This means that radiation pressure noise is largest at low

frequencies, and falls off at higher frequencies.

Using 1.5 and including the input field a the output fields are given by:

$$\begin{pmatrix} c \\ d \end{pmatrix} = e^{i(\Phi + \pi/2)} \begin{pmatrix} \sin \phi & \cos \phi \\ \cos \phi & -\sin \phi \end{pmatrix} \begin{pmatrix} a \\ b \end{pmatrix} \quad (1.44)$$

The signal on the photo-detector is proportional to $c^\dagger c$:

$$c^\dagger c = a^\dagger a \sin^2 \phi + (b^\dagger a + a^\dagger b) \frac{\sin 2\phi}{2} + b^\dagger b \cos^2 \phi \quad (1.45)$$

Using the same operating point as in Section 1.1, $\phi = \pi/2 + \Delta$, we can make the small angle approximation for Δ . We will also write the operators as the sum of a constant and fluctuating part: $\bar{b} + \delta b$, and $a = \delta a$ since only quantum fluctuation enter from the dark port. Assuming again that the laser is in a coherent state we can replace \bar{b} with $|\beta|e^{i\theta_b}$. Dropping terms that are products of fluctuations we get:

$$c^\dagger c = - \left(\Delta + \frac{Lh_+}{2} \right) |\beta| X_a(-\theta_b) + \left(\Delta + \frac{Lh_+}{2} \right)^2 (|\beta|^2 + |\beta| X_b(-\theta_b)) \quad (1.46)$$

Although we have assumed that Δ is small, we have assumed that β is large, so we will not drop the second term, but we can drop the last term which goes as $\Delta^2 |\beta|$. The photo-current at the dark port has a constant part due to the offset from the dark fringe: $|\beta|^2 \Delta^2$, and noise due to the fluctuations entering from the dark port. The fluctuations that cause shot noise are in an orthogonal quadrature to those that cause radiation pressure noise.

To understand how sensor noise limits the sensitivity of a measurement, we need to calibrate the sensor noise in terms of gravitational wave strain.

$$\text{shot noise limited sensitivity} = \frac{\text{quantum noise of } c^\dagger c}{\frac{d(c^\dagger c)}{d h_+}} \propto \frac{1}{|\beta|} \quad (1.47)$$

The sensitivity of a simple Michelson interferometer to gravitational waves scales with the input power, shown in 1.7, meaning that the shot noise limited sensitivity is inversely propor-

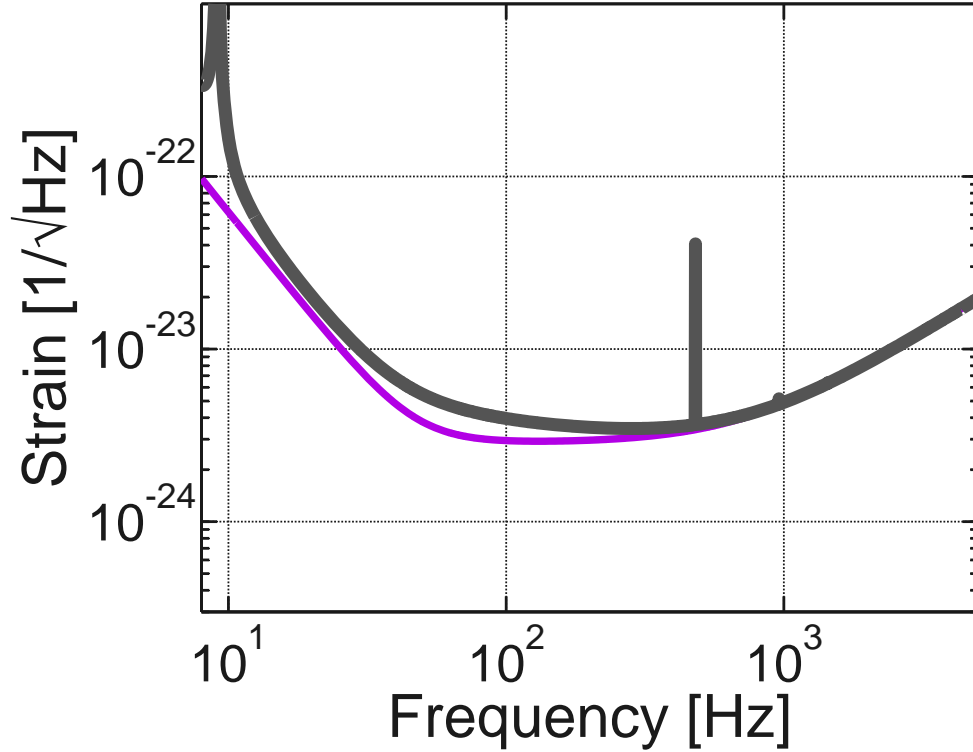


Figure 1-7: Quantum noise limited sensitivity of Advanced LIGO, shown by the purple trace. The shot noise dominates above 100 Hz, calibrated in units of gravitational wave strain the shot noise limit increases with frequency above the arm cavity pole. The gray trace shows the design sensitivity, which is limited by quantum noise at most frequencies in the detection band.

tional to the laser amplitude. By increasing the laser power, the shot noise limited sensitivity can be improved, while increasing the quantum radiation pressure noise. Advanced LIGO has increased the laser power to lower the shot noise limit, and increased the mirror masses to counteract the increased level of radiation pressure noise. The laser power used will test the limits of available technologies, and further increases in laser power and mirror mass will be difficult and expensive.

The LIGO interferometers also include Fabry-Perot arm cavities, which effectively increase the arm length. For an interferometer with Fabry-Perot arms the calibration of power

at the antisymmetric port in gravitational wave strain has a frequency dependence [5]:

$$\frac{\text{quantum noise of } c^\dagger c}{\frac{d(c^\dagger c)}{d h_+}} \propto \frac{1 + i2\Omega\tau_s}{|\beta|} \quad (1.48)$$

where τ_s is the storage time of the arm cavities. This means that the spectrum of quantum noise calibrated in units of gravitational wave strain has a positive slope above the half width of the arm cavities, as shown for Advanced LIGO in 1-7. Once Caves clarified that the vacuum fluctuations at the dark port cause the dominant quantum noise in an interferometer, he suggested that the noise could be reduced by replacing the vacuum fluctuations with a state with a smaller variance in one quadrature.

1.4 Squeezed States

The uncertainty principle places a minimum on the product of the quadrature variances. For a Gaussian state this is a minimum area in phase space that the state must occupy. However, the uncertainty principle places no minimum on the variance of either quadrature alone, so it is possible to have states with smaller variance in one quadrature than a coherent state, as long as the variance of the orthogonal quadrature is larger. These states are called quadrature squeezed states, and in phase space they resemble a coherent state which has been squeezed.

1.4.1 Two Photon Coherent States

Yuen considered states that are eigenstates of a linear combination of the annihilation and creation operators [17]:

$$b|\beta\rangle = (\mu a + \nu a^\dagger)|\beta\rangle = \beta|\beta\rangle \quad (1.49)$$

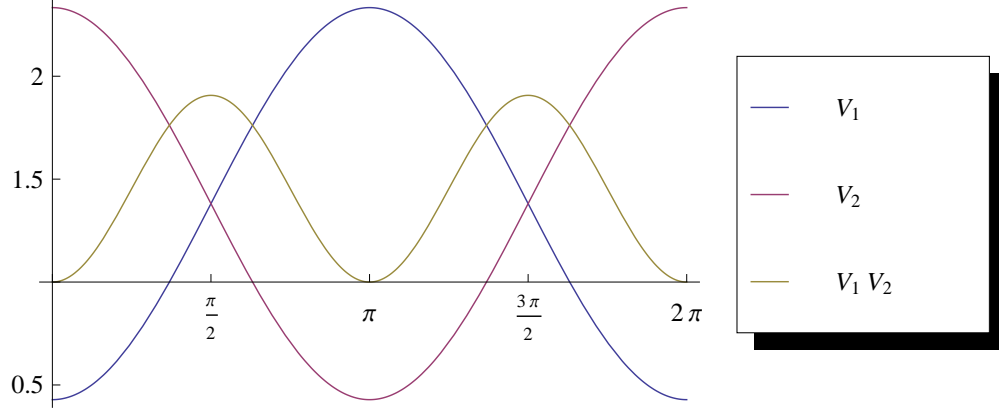


Figure 1-8: Quadrature variances of two photon states with $\beta = 0$ and $\tanh |\zeta| = 0.4$ as θ varies. When the variance of one quadrature is less than one, the other quadrature has increased variance. When θ is an integral multiple of π , the state is a minimum uncertainty state, and the product of the variances in the two quadratures is one.

where $|\mu|^2 - |\nu|^2 = 1$ and $|\nu/\mu| < 1$. He called these states two-photon coherent states, the coherent states discussed in 1.2.5 are a special case when $\nu = 0$. This operator has the same commutation relation as the annihilation and creation operators: $[b, b^\dagger] = (|\mu|^2 - |\nu|^2)[a, a^\dagger] = 1$. By writing a and a^\dagger in terms of b and b^\dagger and using the eigenvalue equation, it is straightforward to find expectation values for the quadrature operators and their variances on these states. We will use the notation:

$$\tanh |\zeta| = \left| \frac{\nu}{\mu} \right| \quad \frac{\nu}{\mu} = \left| \frac{\nu}{\mu} \right| e^{i\theta} \quad \zeta = |\zeta| e^{i\theta} \quad (1.50)$$

As shown in 1-8 these states can have a variance less than the coherent state, and can be minimum uncertainty states. When $\theta = 0$ the variances are:

$$V_1 = \frac{1 - \tanh \zeta}{1 + \tanh |\zeta|} = e^{2|\zeta|} \quad (1.51)$$

$$V_2 = \frac{1 + \tanh \zeta}{1 - \tanh |\zeta|} = e^{-2|\zeta|} \quad (1.52)$$

1.4.2 Photon statistics

The eigenstates of the generalized number operator $b^\dagger b = m |m\rangle$ are generated from the generalized zero state:

$$|m\rangle = \frac{b^{\dagger m}}{\sqrt{m!}} |0\rangle_b \quad b |0\rangle_b = 0 \quad (1.53)$$

An argument exactly analogous to the one leading to 1.31 and 1.32 shows that measurements of the generalized number operator $b^\dagger b$ on the two photon coherent states will result in a Poisson distribution, just like measurements of the number operator on a coherent state [10]. We can write the two photon coherent state in terms of number states following the same procedure used in 1.2.5 to find a recursion relation [10]:

$$c_n = \frac{\beta c_{n-1} - \nu \sqrt{n-1} c_{n-2}}{\mu \sqrt{n}} \quad (1.54)$$

The normalization $\sum |c_n|^2 = 1$ gives $|c_0| = 1/\sqrt{\cosh|\zeta|}$. The coefficients for the generalized zero state $|0\rangle_b$ are found by setting $\beta = 0$.

$$c_{2n+1} = 0$$

$$c_{2n} = \left(\frac{-\nu}{\mu}\right)^n \sqrt{\frac{(2n-1)!!}{(2n)!!}} c_0 = \left(\frac{-\nu}{2\mu}\right)^n \frac{\sqrt{(2n)!}}{n! \sqrt{\cosh \zeta}} \quad (1.55)$$

This is a state with an even number of photons. The state $|1\rangle_b = b^\dagger |0\rangle_b$, and any odd generalized number state includes only odd photon number states.

1.4.3 Squeezing operator

To find the generator of these states we can follow a procedure similar to the one used to show that the displacement operator generates coherent states:

$$|0\rangle_b = \sum_{n=0}^{\infty} c_0 \left(\frac{-\nu}{2\mu}\right)^n \frac{a^{\dagger 2n}}{n!} |0\rangle = c_0 e^{(-\nu a^{\dagger 2}/2\mu)} |0\rangle \quad (1.56)$$

We can re-write the vacuum state as:

$$|0\rangle = (\cosh |\zeta|)^{-a^\dagger a} e^{(\tanh |\zeta| e^{-i\theta} a^2/2)} |0\rangle \quad (1.57)$$

using the fact that $a|0\rangle = 0$. So that our generalized ground state has become:

$$\begin{aligned} |0\rangle_b &= e^{(-\tanh |\zeta| e^{i\theta} a^{\dagger 2}/2)} (\cosh |\zeta|)^{-(a^\dagger a + 1/2)} e^{(\tanh |\zeta| e^{-i\theta} a^2/2)} |0\rangle \\ &= S(\zeta) |0\rangle \end{aligned} \quad (1.58)$$

This operator $S(\zeta)$ has been shown [6] to be the same as the unitary squeezing operator $S(\zeta) = \exp((\zeta^* a^2 - \zeta a^{\dagger 2})/2)$. The squeezed coherent states are generated by [16]:

$$|\alpha, \zeta\rangle = D(\alpha) S(\zeta) |0\rangle \quad (1.59)$$

The squeezed state with $\alpha = \mu\beta - \nu\beta^*$ is equivalent to the two photon coherent state $|\beta\rangle$ [16, p19].

The Q representation quasi-probability distribution of the pure squeezed state $D(\alpha_1) S(\zeta) |0\rangle$ is [9]:

$$\begin{aligned} Q(\alpha) &= \frac{1}{\pi \cosh |\zeta|} \exp \left(-|\alpha|^2 - |\alpha_1|^2 + \frac{\alpha_1^* \alpha + \alpha_1 \alpha^*}{\cosh |\zeta|} \right. \\ &\quad \left. - \frac{\tanh |\zeta|}{2} [e^{i\theta} (\alpha_1^{*2} - \alpha^{*2}) + e^{-i\theta} (\alpha_1^2 - \alpha^2)] \right) \end{aligned} \quad (1.60)$$

Figure 1-9 shows quasi-probability distributions for a few squeezed states. In phase space these states look similar to the coherent and vacuum states, but they have been squeezed.

1.4.4 Squeezed vacuum state

The term squeezed vacuum state is used to refer to the state $S(\zeta) |0\rangle$, which has a equivalent generalized zero state with $\beta = 0$. The quadrature operators are proportional to the electric (X_1) and magnetic (X_2) field amplitudes, and the expectation values for a two photon

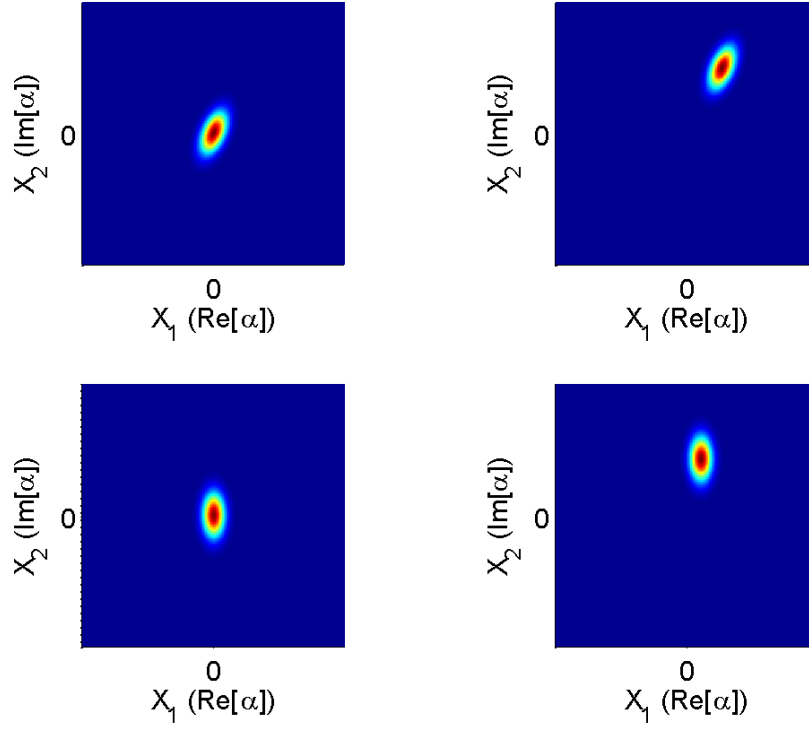


Figure 1-9: Squeezed states

coherent state are:

$$\langle \beta | X_1 | \beta \rangle = 2 \operatorname{Re}[\mu^* \beta - \nu \beta^*] \quad (1.61)$$

$$\langle \beta | X_2 | \beta \rangle = -2 \operatorname{Im}[\mu^* \beta - \nu \beta^*] \quad (1.62)$$

when $\beta = 0$ these are zero just as for the ground state. These states are vacuum states in the sense that the average amplitude is zero. We cannot identify a quadrature operator as an amplitude or phase quadrature operator for either the ground state or the squeezed vacuum states, since we do not have the phase of the coherent amplitude to use as a reference.

Although the squeezed vacuum states have zero amplitude, they do contain more photons than the ground state. The average energy of the state is proportional to the photon number

expectation value:

$$\hbar\omega\left(\frac{1}{2} + \langle\beta| a^\dagger a |\beta\rangle\right) = \hbar\omega\left(\frac{1}{2} + |\nu|^2 + (|\mu|^2 + |\nu|^2)|\beta|^2 - 2\text{Re}[\nu^* \mu^* \beta^2]\right) \quad (1.63)$$

For a squeezed vacuum state this is $\hbar\omega(|\nu|^2 + 1/2) = \hbar\omega(\sinh^2 |\zeta| + 1/2)$. The ground state is the minimum energy state where $\nu = \zeta = 0$. The energy of a squeezed state must be larger than that of the ground state, simply because a squeezed state is different from the ground state. A pure traveling wave squeezed state with 15 dB of squeezing, meaning that $10 \log_{10} V = -15$ for one quadrature, has 7.4 photons per second, or 1.4 attoWatts more power than the vacuum fluctuations. For any practical purpose, we can say that there is no power in a squeezed beam. Although these states have higher energy than the vacuum state, we will call them squeezed vacuum states, they are vacuum states in the sense that they have no coherent amplitude.

Bibliography

- [1] Benjamin Buchler. *Electro-Optic Control of Quantum Measurements*. PhD thesis, Australian National University, September 2001.
- [2] Carlton M. Caves. Quantum-mechanical noise in an interferometer. *Phys. Rev. D*, 23:1693–1708, Apr 1981.
- [3] Carlton M. Caves and Bonny L. Schumaker. New formalism for two-photon quantum optics. i. quadrature phases and squeezed states. *Phys. Rev. A*, 31:3068–3092, May 1985.
- [4] M. J. Collett and C. W. Gardiner. Squeezing of intracavity and traveling-wave light fields produced in parametric amplification. *Phys. Rev. A*, 30:1386–1391, Sep 1984.
- [5] B P Abbott for the LSC. Ligo: the laser interferometer gravitational-wave observatory. *Reports on Progress in Physics*, 72(7):076901, 2009.
- [6] R. Friedberg. The squeezing operator in quasinormal form. *Laser Physics*, 12(8):1171–1176, 2002.
- [7] C. W. Gardiner and M. J. Collett. Input and output in damped quantum systems: Quantum stochastic differential equations and the master equation. *Phys. Rev. A*, 31:3761–3774, Jun 1985.
- [8] J. C. Garrison and R. Y. Chiao. *Quantum Optics*. Oxford University Press, Oxford, 2008.
- [9] Christopher C. Gerry and Peter L. Knight. *Introductory Quantum Optics*. Cambridge University Press, Cambridge, 2005.
- [10] Richard W. Henry and Sharon C. Glotzer. A squeezed-state primer. *American Journal of Physics*, 56(4):318–328, 1988.
- [11] Kirk McKenzie. *Squeezing in the Audio Gravitational Wave Detection Band*. PhD thesis, Australian National University, February 2008.
- [12] Bonny L. Schumaker and Carlton M. Caves. New formalism for two-photon quantum optics. ii. mathematical foundation and compact notation. *Phys. Rev. A*, 31:3093–3111, May 1985.

- [13] Marlan O. Scully and M. Suhail Zubairy. *Quantum Optics*. Cambridge University Press, Cambridge, UK, 1997.
- [14] Anthony E Siegman. *Lasers*. University Science Books, Mill Valley, CA, 1986.
- [15] Nicolas Smith-Lefebvre. *Techniques for Improving the Readout Sensitivity of Gravitational Wave Antennae*. PhD thesis, Massachusetts Institute of Technology, June 2012.
- [16] D F Walls and Gerard J Milburn. *Quantum Optics*. Springer, Berlin, 2008.
- [17] Horace P. Yuen. Two-photon coherent states of the radiation field. *Phys. Rev. A*, 13:2226–2243, Jun 1976.